Atomic and electronic structures of 4*d* transition-metal nitrides

R. de Paiva* and R. A. Nogueira

Departamento de Física, Universidade Federal de Minas Gerais, CP 702, 30123-970 Belo Horizonte, MG, Brazil

J. L. A. Alves

Departamento de Ciências Naturais, Universidade Federal de São João del Rei, CP 110, 36301-160 São João del Rei, MG, Brazil

A systematic theoretical study of the zinc-blende-type 4*d* transition-metal nitrides, which has not yet been synthesized, is performed in order to anticipate their electronic properties. Calculations were carried out by means of spin-polarized first-principles full-potential linearized augmented plane-wave calculations using the local spin-density approximation. Lattice constants, bulk moduli, cohesive and formation energies, charge distributions, energy band structures, and density of states are reported, and trends are discussed.

I. INTRODUCTION

Nowadays, the advancements in the *ab initio* quantum-mechanical calculations of the atomic and electronic structures allow the theoretical modeling of new materials which permits the prediction of their properties and the suggestion of new syntheses. On the other hand, the III-nitride compounds, in the zinc-blende phase, have deserved great experimental and theoretical attention in connection with their potential applications in optoelectronics and spintronics.[1,2] Previously, we have studied the dilute magnetic semiconductors $Ga_{1-x}Mn_xN$ and $Al_{1-x}Mn_xN$ and the related compound MnN in the zinc-blende phase.[2] In the present work we study the 4*d* transition-metal nitrides, in the zinc-blende phase, in a perspective to integrate their structural, electronic, and magnetic properties to those of the III-nitride compounds in the zinc-blende phase. The 3*d* transition-metal nitrides have deserved more experimental and theoretical attention than the 4*d* transition-metal nitrides. The ScN, TiN, VN, and CrN compounds have been synthesized in the fcc (NaCl-type) structure. ScN was identified as a semiconductor;[3] TiN and VN as superconductors.[4] FeN films synthesized by sputtering appear, depending on the experimental conditions, either in the NaCl structure or in the ZnS (zinc-blende) structure.[5] CoN films, in the zinc-blende phase have also been synthesized.[6] On the theoretical side, *ab initio* calculations show that the 3*d* transition-metal nitrides usually exhibit a NaCl structure with lower energy than the zinc-blende structure.

Concerning the experimental investigations on the 4*d* transition-metal mononitrides, they have been dedicated mainly to MoN, NbN, YN, and ZrN: MoN, which crystallizes in the hexagonal phase, was the object of the earlier studies due to its potential superconductor properties;[7] the electronic properties of cubic and hexagonal NbN films has been studied in connection with their functional mechanical, electrical, superconductor, and optical properties;[8–14] YN in the form of thin films has deserved recent attention due to its potential use in YN/GaN heterostructures or YGaN alloys;[15–18] many studies of hard cubic zirconium nitride thin films are related to wear applications.[19] On the other hand, some *ab initio* calculations have been carried out for the 4*d* transition-metal nitrides series in the fcc structure.[7,20,21] In the present work our aim is to carry out *ab initio* calculations for the zinc-blende (ZB) phase of the 4*d* transition-metal nitrides; for completeness we compare our results to those existing in the literature for the other phases. These hypothetical systems, perhaps not realizable in their isolated forms, could be feasible to occur as inclusions inside the zinc-blende phases of other systems, for example, inside III-nitride compounds and their alloys. It has turned out to be a commonplace preparation, in a reproducible way, of compounds in structures which are not the most stable, and, actually, nonequilibrium phase diagrams have turned to be a subject of research. Based on these arguments we consider appropriate the theoretical study of 4*d* transition-metal nitrides in the zinc-blende phase, which have not yet been fabricated in the laboratory. As we stressed before, the goal of the present work is to investigate, in detail, the electronic structure of the 4*d* transition-metal nitrides in connection to their possible applications related to the recent development of the technology of semiconductors based on III-nitride in the zinc-blende phase.[22] We study the (4*d*-TM)N materials, in which notation 4*d*-TM refers to a transition metal having 4*d* electrons [Y($Z=39$), Zr($Z=40$), Nb($Z=41$), Mo($Z=42$), Tc($Z=43$), Ru($Z=44$), Rh($Z=45$), Pd($Z=46$), Ag($Z=47$)], and examine the trends of their structural, electronic, and magnetic properties.

As a possible guide for future experimental attempts to stabilize the zinc-blende phase of the (4*d*-TM)N compounds, we list some experimental methods already used in the production of MoN samples in different crystalline phases:[7] (i) by passing a flux of ammonium gas over metal Mo powder heated to 700–900 °C;[23] (ii) nitridation of Mo films using an ammonium flux;[24] (iii) nonequilibrium techniques for growing stabilized zinc-blende structures;[7] (iv) sputtering of Mo using N_2, CN, or ammonium vapor;[25] (v) evaporation by electron beam and vapor deposition including organometallic transport;[26] (vi) ionic implantation of nitrogen atoms in Mo films followed by annealing;[27] (vii) shock compression over MoN samples in other phases than the zinc blende;[28,29] (viii) epitaxial growth over GaN or AlN substrates; (ix) growing of sandwiched structures, under high pressures, for example, the structure NbN-MoN-NbN; (x) ion implantation, using high-energy transition-metal ions.[27] It is worth mentioning that very recently, the noble metal nitride PtN, in the zinc-

TABLE I. Plane-wave cutoffs K_{max} and the muffin-tin radii R_{mt} adopted in the calculations. The number of k points used in the irreducible part of the Brillouin zone is 72 in all cases.

System	K_{max}	R_{mt}(bohr)
YN	4.62	$R_Y = 2.00$, $R_N = 1.68$
ZrN	4.85	$R_{Zr} = 1.94$, $R_N = 1.64$
NbN	4.48	$R_{Nb} = 2.10$, $R_N = 1.74$
MoN	5.58	$R_{Mo} = 1.70$, $R_N = 1.42$
TcN	5.53	$R_{Tc} = 1.70$, $R_N = 1.42$
RuN	5.56	$R_{Ru} = 1.70$, $R_N = 1.42$
RhN	5.51	$R_{Rh} = 1.70$, $R_N = 1.42$
PdN	5.52	$R_{Pd} = 1.70$, $R_N = 1.42$
AgN	4.96	$R_{Ag} = 1.90$, $R_N = 1.60$

blende phase, has been synthesized[30] at pressures up to 50 GPa using laser heated diamond-anvil-cell techniques by Gregoryanz *et al.*[30] This achievement opens the possibility that, by means of high-pressure based techniques, other transition-metal nitrides may be synthesized in the zinc-blende phase.

II. METHOD OF CALCULATION

We carry out all-electron, self-consistent, first-principles, spin-polarized calculations using the full-potential linear augmented plane-wave (FP-LAPW) method within the local spin-density approximation (LSDA).[35] In particular we use the FP-LAPW method as implemented in the WIEN2K code.[36] We have included scalar-relativistic effects for all valence states (including the 4d-TM states). Core states are calculated fully relativistically, retaining only the spherical part of the potential. The effects of exchange correlation are treated using the Ceperley-Alder data[37] for the electron gas exchange term and their parametrization by Perdew and Wang.[38] The valence part is treated with the potential expanded into spherical harmonics up to $l=6$. The valence wave functions inside the spheres are expanded up to $l=10$. In all cases we use an APW+lo orbital[39,40] type basis with additional local orbital for the TM 4s and 4p semicore states. The muffin-tin radii (R_{mt}), k-point set, and plane-wave cutoffs K_{max} used in the calculation are listed in Table I. We used a zinc-blende structure (space group $\bar{F}43m$) with two atoms in the primitive unit cell to simulate the binary compounds. Self-consistency was achieved by demanding the convergence of both the total energy and the eigenvalues to be smaller than 10^{-6} eV.

III. STRUCTURAL PROPERTIES

The equilibrium lattice constants and the bulk moduli, listed in Table I for the 4d transition-metal nitrides, were obtained by performing total-energy calculations for the two-atom unit cell. The equilibrium lattice constants and the bulk

TABLE II. Lattice constant a_o and *bulk moduli B* for all 4d transition-metal nitrides in the zinc-blende and NaCl structure. a_M is the lattice parameter and B_M is the *bulk modulus* for the 4d transition metal calculated in the fcc structure.

	YN	ZrN	NbN	MoN	TcN	RuN	RhN	PdN	AgN
a_o (Å)	5.19	4.90	4.70	4.58	4.50	4.47	4.51	4.62	4.79
Other works	4.77[a]	4.53[a]	4.36[a]						
(NaCl)	4.85[b]	4.57[b]	4.42[b]						
			4.38[c]	4.25[c]					
Expt.	4.877[a]	4.537[a]	4.392[a]						
		4.61[a]							
B (GPa)	126.19	202.10	260.37	290.17	310.30	307.32	267.85	217.18	149.57
Other works	204[a]	292[a]	354[a]						
(NaCl)	163[b]	264[b]	317[b]						
a_M (Å)	4.88[d]	4.43[d]	4.14[d]	3.95[d]	3.82[d]	3.76[d]	3.78[d]	3.86[d]	4.02[d]
(fcc)							3.76[e]	3.83[e]	
	4.95[f]	4.47[f]	4.20[f]	4.00[f]	3.88[f]	3.83[f]	3.85[f]	3.94[f]	4.11[f]
B_M (GPa)	52.60[d]	104.70[d]	179.80[d]	256.40[d]	299.60[d]	354.80[d]	311.60[d]	201.10[d]	113.10[d]
					313[e]	226[e]			
	40[f]	80[f]	160[f]	230[f]	310[f]	320[f]	210[f]	190[f]	110[f]

[a]FP-LAPW within LDA (Ref. 21).
[b]FP-LAPW within GGA (Ref. 21).
[c]APW within LDA (Ref. 7).
[d]APW within LDA (Ref. 42).
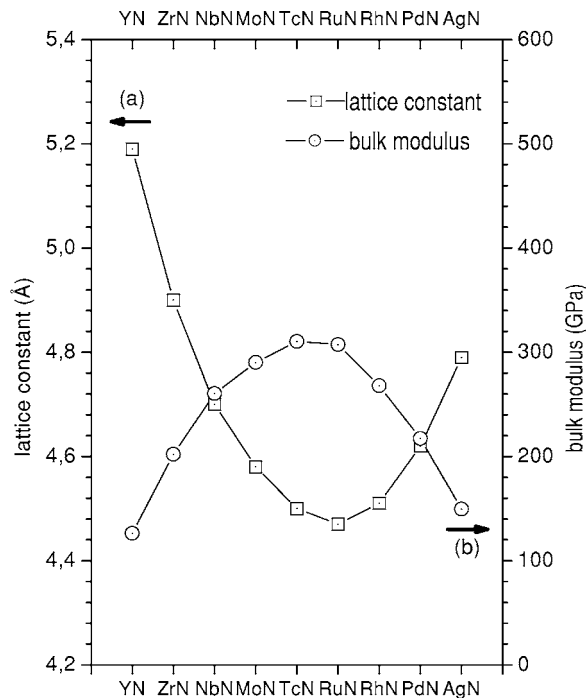[e]FP-LMTO within LDA (Ref. 43).
[f]APW within LDA (Ref. 44).

FIG. 1. The equilibrium lattice constants (a) and bulk moduli (b) of zinc-blende-type structure 4d transiton-metal nitrides.

moduli of those compounds were estimated by fitting the total energies to the Murnaghan equation of states.[41] In Table II we compare our results for the lattice parameter a_o and the bulk modulus B to other theoretical and experimental values in the literature. In this table are also shown the theoretical values a_M and B_M for the pure metals, in the fcc phase, as obtained by Sigalas et al.[42] using the APW-LDA method. As usual in the calculations using the LDA the lattice parameters are expected to be underestimated by 1–2% and the bulk moduli to be overestimated by 10–12%. We display the equilibrium lattice constants and the bulk moduli in Fig. 1 for the (4d-TM)N series, and in Fig. 2 for the pure transition-metals series. We can observe a similar behavior in both series. The variations of a_o, B, a_M, and B_M with the atomic number of the transition metal reflect the fact that the occupation of the d band of the metal increases the strength of the d band, which reaches its maximum in the middle of the series. It is interesting to note that we have obtained larger lattice constants for ZB type than those reported for NaCl type (4d-TM)N.[7,20,21,44,45] This result seems reasonable because in ZB type the N atoms are located at the tetrahedral site of the face-centered-cubic (fcc) structure of the transition-metal atoms, and this site is rather closer to neighboring transition-metal atoms as compared to the octahedral site of the N atoms in the NaCl-type structure. On the other hand, comparing our results for the nitride to those obtained by Sigalas et al.[42] for the pure metals, we observe that, in general, by mixing with nitrogen atoms the transition metals become harder. We can understand this on the basis of a simple reasoning. Both the NaCl and the zinc-blende structures may be considered to be built by introducing N atoms on the octahedral or tetrahedral interstitial sites of the transition-metal face-centered-cubic structure. Therefore the distance be-
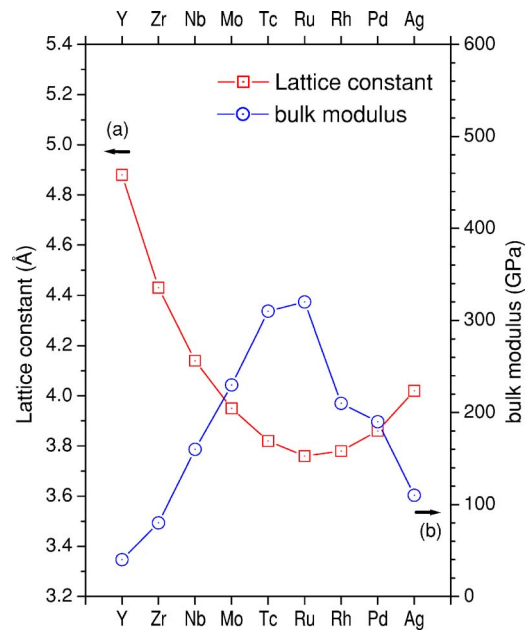

FIG. 2. (Color online) The equilibrium lattice constants (a) and bulk moduli (b) for the pure transition metal in the fcc phase (Ref. 42).

tween the first neighbors is shortened. Obviously the lattice expands but this expansion is not big enough to compensate the decrease of the interatomic distance between the first neighbors. As a result, the metal atoms are less free to move around the equilibrium position, i.e., the compounds become harder than the metals.

Following Lam et al.,[46] who obtained an analytical relation connecting the bulk modulus and the lattice parameter for the III-V compounds using the DFT-LDA formalism, we display in Fig. 3 the bulk moduli values as a function of the first-neighbor distance d. We see that we also can adjust a power law of the form $y = a d^{-b}$ for the (4d-TM)N, in the zinc-blende phase, if we consider separately the first and second halves of the 4d shell: $b = 5.8$ (first half); $b = 10.2$ (second half).
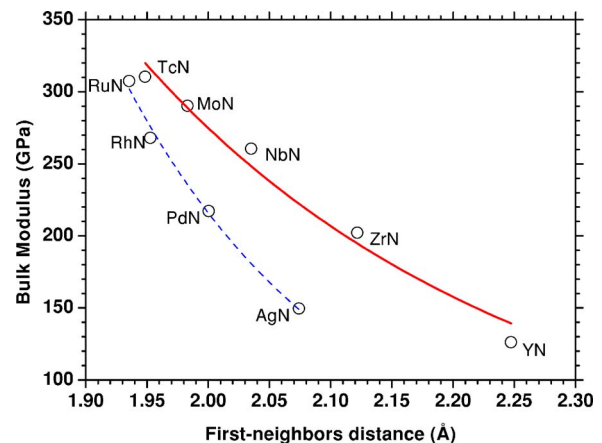

FIG. 3. (Color online) The bulk moduli values as a function of the first-neighbor distance of zinc-blende-type structure 4d transition-metal nitrides.
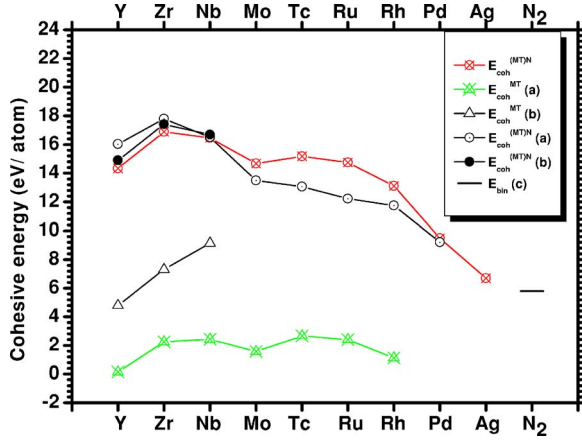
FIG. 4. (Color online) Cohesive energies $E_{coh}^{(4d\text{-}TM)N}$ of the (4d-TM)N in the zinc-blende phase compared to the calculated values for NaCl phase and for the fcc phase of the pure metals, E_{coh}^{TM} (a) Ref. 20, (b) Ref. 42. Also shown is the binding energy of the N_2 molecule E_{bin} (c) Ref. 50.

IV. ELECTRONIC PROPERTIES

### A. Cohesion and formation energies

The theoretical determination of the cohesive properties of the various materials is important because the experimental data are, in general, difficult to be obtained since they depend on high-temperature experiments. We present in Fig. 4 the cohesive energies of the transition-metal nitrides as calculated by means of total-energy calculations for the (4d-TM)N compounds and for the isolated transition-metal and nitrogen atoms,

$$E_{coh} = -\left(E_{(TM)N} - E_{TM} - E_N\right). \qquad (1)$$

The critical point of these calculations are the total atomic energies. Although the computational effort to determine the atomic energies is less than in the case of a compound, it is well known that most of the error involved in the calculation of the cohesive energies is due to the atomic calculations. Besides, the problem is complicated by the fact that the use of Eq. (1), based on the separate determination of the solid and the atomic energies, relies on a cancellation of systematic errors.[20] The atomic energies were obtained using a procedure which is coherent to the solid-state calculations of the (4d-TM)N compounds: the atomic energies were calculated not using an atomic computational code but the FP-LAPW solid state code. We created a fcc box with lattice constant of about 30 bohr having the atom placed at (0,0,0). We used identical parameters as in the compound calculations, but only one k point (Γ-point) and spin polarization. [In order to calculate the total energy of a free atom using periodic boundary conditions, a large unit cell is needed to prevent that an atom from an unit cell interacts with an atom of a neighboring unit cell; the size of the cell depends on the element in question. A common practice is to use only one point in the Brillouin zone, the Γ point, in the total-energy calculations of a free atom.[47] The use of the (0.25, 0.25, 0.25) $2\pi/a$ point can yield a faster convergence of the total energy with the cell size as compared to selecting the Γ

point.[48,49] This behavior is due to the finite size of the unit cell which provokes a band dispersion, i.e., the atomic eigenvalues split and form a band with finite width. To first order the center of the band lies exactly at the position of the atomic eigenvalues. At the Γ point the eigenvalues at the bottom of the band are obtained; if the special point (0.25, 0.25, 0.25) $2\pi/a$ is used instead of the Γ point, the energy of the center of the band is obtained. In the limit of very large unit cell both k points should lead to the same atomic values. In our calculations we use a fcc unit cell with a large side length equal to 30 bohr which is big enough to reach convergence at the Γ point.] In Fig. 4 we compare our values for the cohesive energies to the calculated ones in Refs. 20 and 21 for NaCl phase of the (4d-TM)N and in Ref. 42 for the fcc phase of the pure metals. We verify that the cohesive energies of the (4d-TM)N zinc-blende compounds lie below the values of the NaCl phase at the beginning of the series and above those values from Mo till the end. The values are always higher than those for the corresponding pure metal but exhibit the same qualitative behavior along the series. This behavior can be understood by following the occupation of the nonligand and antiligand states along the density of states (DOS) curves (see Sec. IV B).

We analyzed also the formation energies for the compounds YN, ZrN, and NbN, at the beginning of the series. In doing this we consider the chemical reaction

$$TM(\text{solid}) + \frac{1}{2}N_2(\text{gas}) \rightleftharpoons (TM)N(\text{solid}) \qquad (2)$$
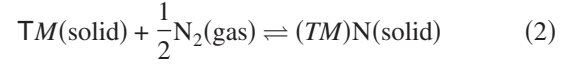
and define

$$E_{for} = E_{tot}^{TM} + \frac{1}{2}E_{tot}^{N_2} - E_{tot}^{(TM)N} = E_{coh}^{(TM)N} - E_{coh}^{TM} - \frac{1}{2}E_{bin}^{N_2}, \quad (3)$$

where $E_{tot}^{(TM)N}$, $E_{tot}^{N_2}$, and E_{tot}^{TM} are, respectively, the total energies of the compound, of the free N_2 molecule, and of the metal; $E_{coh}^{(TM)N}$ and E_{coh}^{TM} are the cohesive energies of the nitride and of the metal, respectively, and $E_{bin}^{N_2}$ is the binding energy of the molecule N_2. In our calculations we adopt $E_{bin}^{N_2} = 11.57$ eV (Ref. 50) and the E_{coh}^{TM} values from Ref. 51. In Fig. 5 we compare our results to those obtained in Ref. 21 for the NaCl phase. In both cases there is a big decrease of the formation energies in passing from ZrN to NbN (~ 2.5 eV). This large decrease in the formation energy of NbN may be linked to the variation of the metal-metal bonds; in the nitrides these bonds are considerably stretched in comparison to the pure metal values [YN(16%), ZrN(19%), NbN(21%)]. What one should expect is that, as the lattice parameter decreases and the bulk modulus increases, at the beginning of the series, the chemical bonding would be stronger, the cohesive energies larger and, consequently, the formation energies larger. However, by Eq. (3), the behavior of the formation energy results from the relative variations of the cohesive energies of the nitrides and transition metals along the series. When going from YN to ZrN, as from Y to Zr, the cohesive energies increase and the formation energy only decreases a little. When going from ZrN to NbN, the cohesive energy decreases while from Zr to Nb the cohesive energy increases, producing a large decreasing of
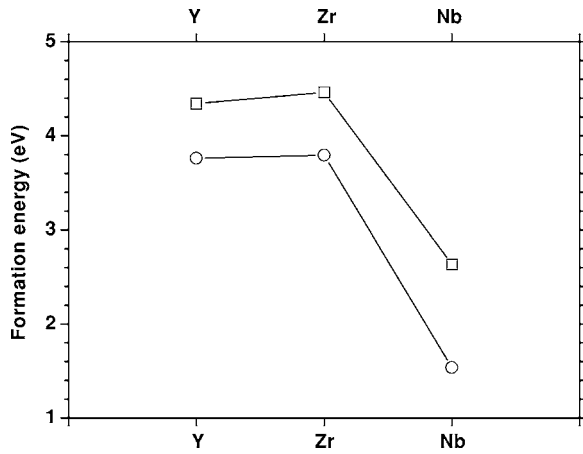
FIG. 5. Formation energies of the (4d-TM)N, in the zinc-blende phase (circles), compared to the calculated ones in Ref. 21 for NaCl phase (squares).

the formation energy. This significant change in the formation energy is thus due to the fact that the cohesive energy of NbN is less than that for ZrN and that for pure Nb is bigger than that for pure Zr. Thus we can assume the following behavior: in the compound, as one goes from the left to the right in the series, the metal-metal distance increases significantly in comparison to the same distance in the pure metal and the system does not have a gain in energy due to the metal-metal bonding. This can be correlated to the fact that the additional electrons, along the nitride series, occupy nonligand states preventing a smaller metal-metal distance.

B. Band structures

The calculated band structures, at the equilibrium lattice constants, are depicted in Fig. 6, which are drawn along symmetry directions in the first Brillouin zone. First, we observe that all materials, in the zinc-blende structure, are metallic, except YN, of which the band structure indicates it is insulating. The band structures exhibit the energy levels originated from atomic states $\Gamma_1(2s\text{-N})$, $\Gamma_{15}^v(2p\text{-N}+4d\text{-TM})$, ligand states, $\Gamma_{12}(4d\text{-TM})$, nonligand states, and $\Gamma_{15}^c(2p\text{-N}+4d\text{-TM})$, antiligand states, at the Γ point. We observe that although the calculations were carried out in the spin-polarized mode, no effective polarization of the states occurred at the equilibrium distances. Fractional occupations occur close to the Fermi level, due to the existence of close empty levels (metallic character), but which leads to no polarization of the materials. We start by analyzing the trends displayed by the 4d atomic orbitals which originate from the transition metals. The 4d atomic states are split into the Γ_{12} and Γ_{15} representations at the Γ point. As the atomic number of the TM increases, the characteristic band separations and widths change as shown in Fig. 7. E_g^1 refers to the energy gap between the lower bands Γ_1 and Γ_{15}^v, E_g^2, between Γ_{15}^v and Γ_{12}, and E_g^3, between Γ_{12} and Γ_{15}^c. $E(\Gamma_{15}^v-\Gamma_1)$ refers to the energy difference between the Γ_{15}^v and Γ_1 levels at the Γ point; $E(\Gamma_{12}-\Gamma_{15}^v)$ and $E(\Gamma_{15}^c-\Gamma_{12})$ have analogous meanings. These energy gaps are direct and occur always at the X point of the Brillouin zone. In order to obtain a deeper in-

sight into the changes in the electronic band compositions we give the total and partial density of states in Fig. 8, where the assignments of the ligand, antiligand, and nonligand character of the electronic states of the (4d-TM)N compounds are also shown. The DOS for all systems lies mainly in four energy regions: (i) the lowest region stemming mainly from N-2s states; (ii) the region at the bottom of the valence-band complex, originating from 5s-TM and 2p-N states; (iii) the region at the top of the valence-band complex. This region, except for YN, is cut by E_F, and is mainly due to 4d-TM states mixed with some 2p-N states; (iv) the energy region just above E_F dominated by unoccupied 4d transition-metal states. It can be seen that the 2p-N states hybridize strongly with the 4d-TM states. Moreover, along the series, the d character of the valence band increases steadily with increasing atomic number. We consider two main factors existing in the formation of the electronic structures of the (4d-TM)N compounds in the zinc-blende phase. The first one is the expansion of the face-centered-cubic lattice of the transition metal due to the insertion of the nitrogen atoms at the tetrahedral interstitial sites. The second one is the interaction between the 4d-TM electrons and the 2p-N electrons. With regard to the pure metal, the largest contribution to its cohesive energy is the formation of the d band from the atomic 4d orbitals.[42] If the bond length in the solid metal would be increased, the width of the d band should decrease, and its contribution to the stability of the system should decrease. The loss of stability regarding the pure metal would be larger, the larger the expansion. On the other hand, when the atoms are put closer, their states are mixed and form ligand and antiligand hybrids. This is the typical interaction which leads to the molecular bond and to the formation of energy bands in solids. When forming a compound between the 4d transition metal and nitrogen, which has the s-p valence shell, there is hybridization among these states, and, consequently, the formation of ligand, antiligand, and nonligand hybrids. A ligand hybrid is more strongly bound than any of the states from which it is formed, as opposed to an antiligand hybrid. In a specific crystalline structure, not all of the d states have the right symmetry to form hybrids, like the $e(\Gamma_{12})$ states in the zinc-blende structure. This fact leads to the nonligand states in the compounds, of which energies are close to the d-band energies of the pure metals. In Figs. 8 and 9 we identify the ligand (Γ_{15}^v), antiligand (Γ_{15}^c), and nonligand states (Γ_{12}). The total ligand-antiligand complex is wider than the d band of the corresponding transition metal. The variations of the bandwidths across the series reflect the variations of the equilibrium volume. The bandwidth $\Delta\Gamma_{15}^v$, which reflects the 4d-sp interaction, increases as the (4d-TM)N distance decreases, reaches a maximum value at the center of the series (Tc), and decreases along the second half of the series. $\Delta\Gamma_{12}$, which reflects the nonligand next-nearest-neighbor TM-TM interactions is, in general, smaller than $\Delta\Gamma_{15}^v$ and has an analogous behavior along the series. On the other hand, as the 4d shell is occupied, the equilibrium volume initially decreases, because of the filling of the nonligand states, and then increases due to the filling of the antiligand states. This leads to minimum volume around the half filled 4d shell. The YN compound has a total of eight
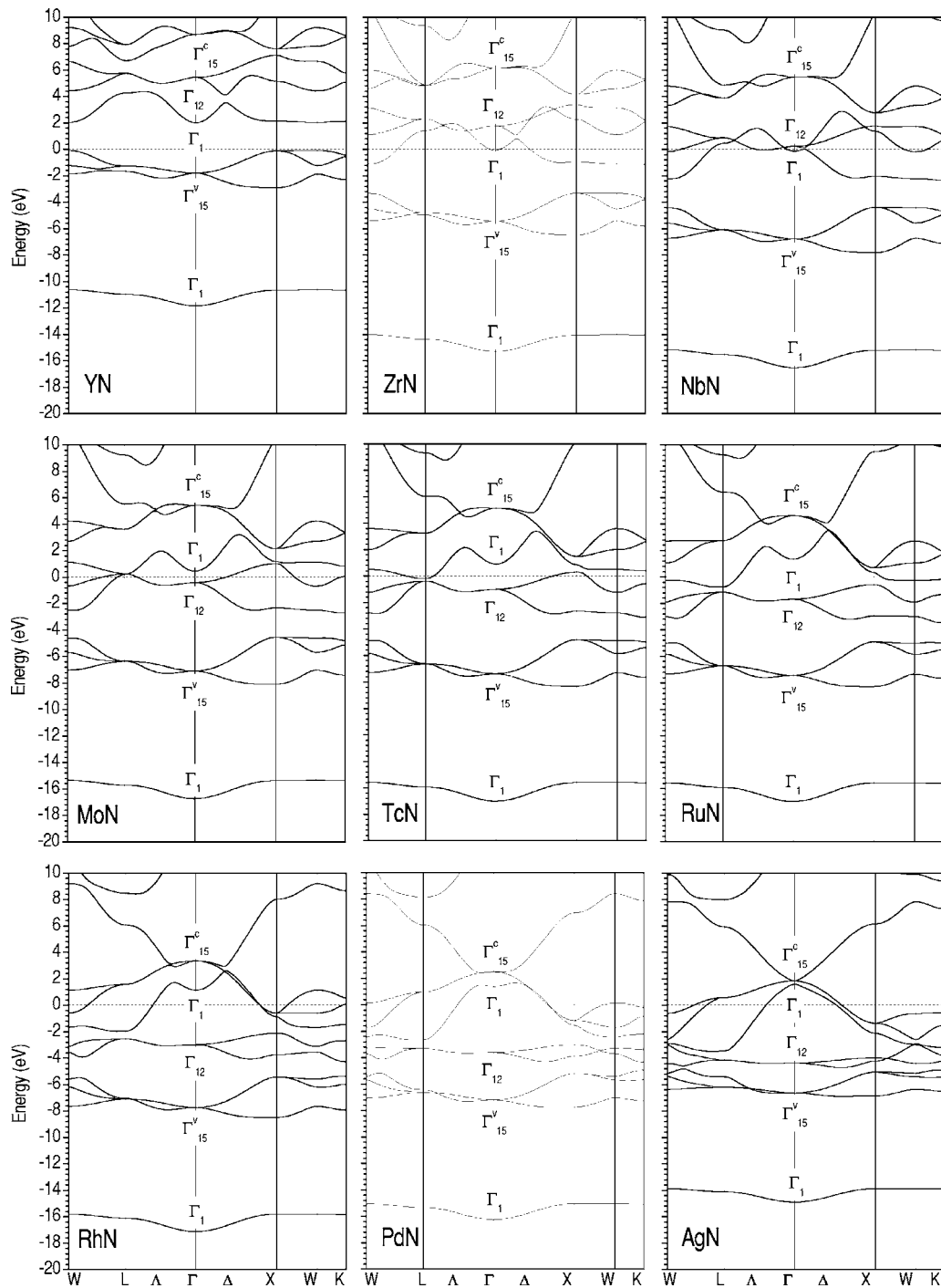
FIG. 6. Band structure for zinc-blende $4d$ transition-metal nitrides at the LDA minimum total energy. The horizontal line denotes the position of the Fermi energy.

valence electrons per unit cell, which is enough to fill all ligand bands Γ_1 and Γ_{15}^v (Figs. 8 and 9). Starting from this compound, the addition of new electrons fills successively the ligand Γ_1 band and the nonligand band Γ_{12}, which is full for RuN. From this compound, new electrons fill antiligand states of the Γ_{15}^c band; at the same time the equilibrium volume increases. The bandwidths indicate the degree of overlap of the atomic orbitals, which is reflected in the fact that the largest bandwidths occur in the middle of the series. Turning our attention to the density of states, we observe that

we can distinguish between ionic and covalent characters of the bonds in these compounds. If the bond is strongly ionic, there is only a small mixture of the atomic states of the two components of the compound and the DOS curves are very different in the two atomic sites. If the bond is mainly covalent, the atomic states are very much mixed and the DOS curves, at both atomic sites are very similar. These features may be observed comparing in Figs. 8 and 9 the contributions of the $2p$-N and $4d(t_2)$-TM orbitals to the total DOS; their shapes seem to be replicated. On the other hand, the
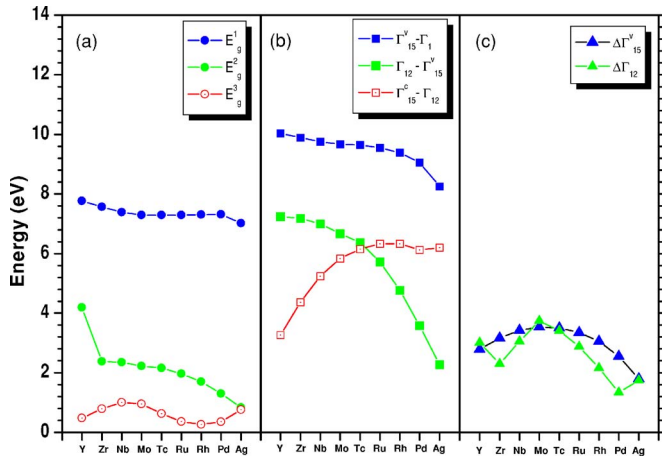
FIG. 7. (Color online) Characteristic band separations and bandwidths.

contributions of the nonligand orbitals, $4d(e)$-TM are just those which do not present a mirrored peak at the nitrogen site.

C. Charge distribution

In order to analyze the net charges of the atoms in the unit cell we adopt an arbitrary procedure which we think is accurate enough for a qualitative discussion of the charge transfer between the transition metal and the nitrogen along the series. Table III displays the total charges inside the atomic spheres and in the interstitial region (between the atomic spheres), in the unit cell, in accord with the geometry adopted in the FP-LAPW method for the generation of the basis set functions. We attribute net charges to the atoms by distributing the charges contained in the interstitial region among the atoms, proportionally to the volumes of the atomic spheres. These charges are added to the charges inside the atomic spheres. In this way we attribute an average charge of $\sim+0.6|e|$ to the metals, and, naturally, a $\sim-0.6|e|$ charge to the N atom. This means that we attribute some ionic character to the $(4d$-TM)N compounds. Earlier we have also attributed to these materials a covalent character due to the strong hybridization between the N and the transition-metal states, according to the density-of-states analyses; however, as we see there is also an ionic compo-
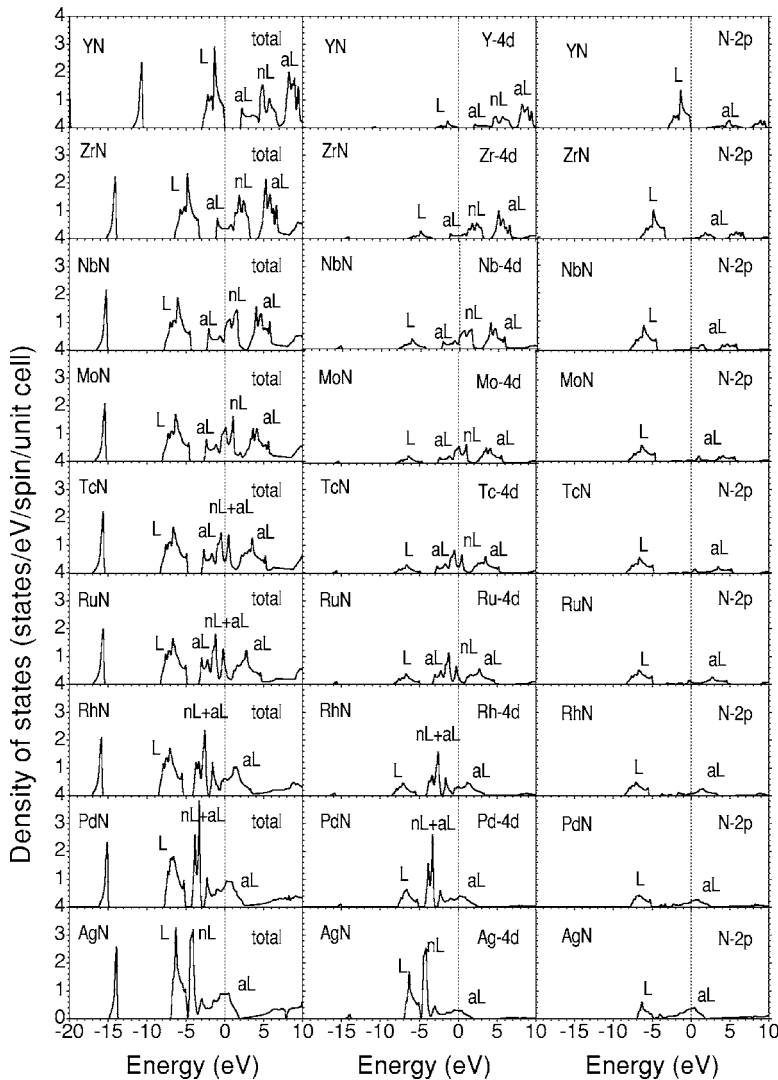

FIG. 8. Total and partial density of states for the zinc-blende $4d$ transition-metal nitrides at the LDA minimum total energy. The vertical line denotes the position of the Fermi energy. The ligand states are denoted by L, antiligand by aL, and nonligand by nL.
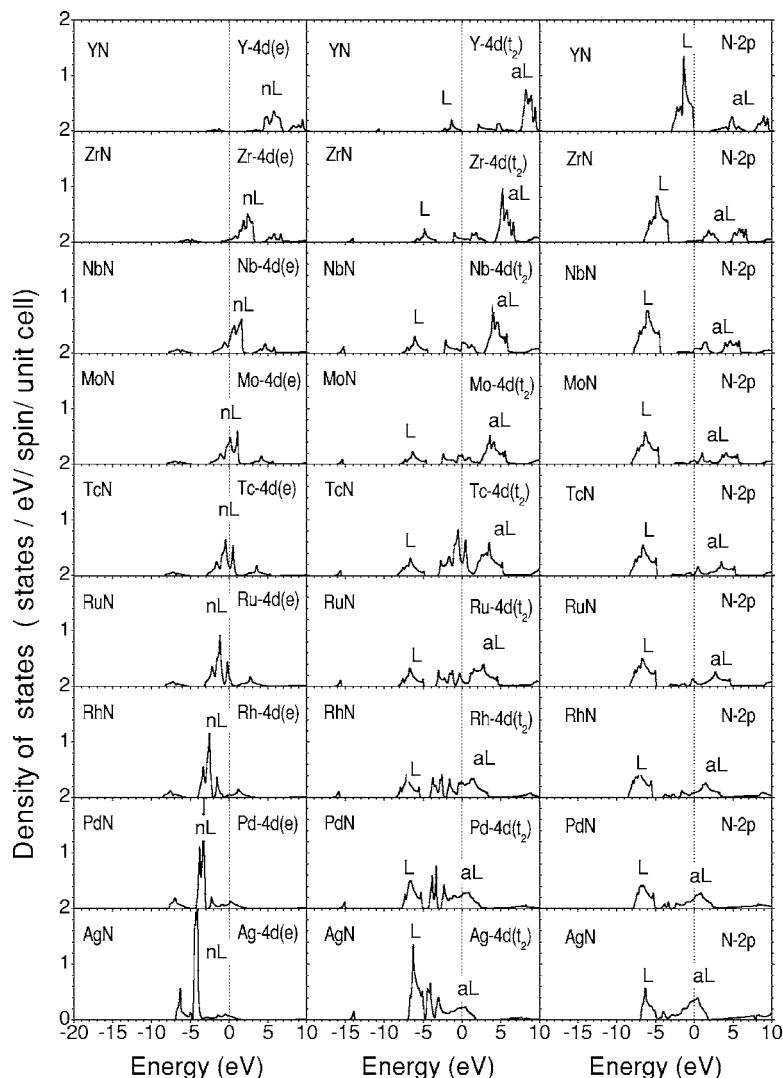
FIG. 9. Partial density of states for $4d(e)$-TM, $4d(t_2)$-TM, and $2p$-N. The vertical line denotes the position of the Fermi energy. The ligand states are denoted by L, antiligand by aL, and nonligand by nL.

nent with a significant charge transfer to the more electronegative atom, N, as well as a clear metallic nature (except for YN). This analysis is also consistent with the fact that the Fermi level lies below the top of the $4d$-p band complex, resulting in more occupied ligand states than antiligands states; we can expect, then, that there will be charge transfer to the atoms having more strongly bonded orbitals, i.e., from the transition metals to the nitrogen (hybrid ligand orbitals have larger amplitudes over atoms having more bound orbit-

als, while the antiligands are more concentrated on the atoms having less bound orbitals). On the other hand, the presence of the N in the compound displaces the transition-metal $5s$ states to far above the $4d$ states energies. The result is that there is only a small hybridization of the $5s$ states with the $4d$ and $2p$-N states in the compound; this gives rise to more "pure" d states in the compound than in the pure metal. This reduced hybridization $5s$-$4d$ is consistent with the $5s$ electron transfer from the metal to N.

TABLE III. Total charges, in the unit cell (in units of the electron charge) contained in the atomic spheres and in the interstitial region, $Q(4d$-TM$)$, $Q(N)$, $Q(I)$, respectively. $Q^{\star}(4d$-TM$)$ and $Q^{\star}(N)$ are the net charges attributed to the atoms. $Z(TM)$ is the atomic number of the transition metal.

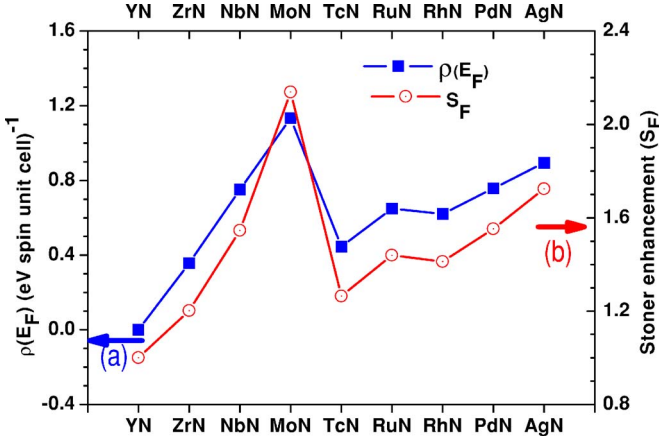|	YN	ZrN	NbN	MoN	TcN	RuN	RhN	PdN	AgN
$Q(4d$-TM$)$	35.54	36.20	37.82	37.21	38.35	39.48	40.63	41.78	43.86
$Q(N)$	6.17	6.13	6.51	5.41	5.39	5.36	5.31	5.25	5.77
$Q(I)$	4.29	4.67	3.67	6.38	6.26	6.15	6.06	5.97	4.37
$Q^{\star}(4d$-TM$)$	38.30	39.21	40.18	41.32	42.38	43.45	44.53	45.62	46.67
$Z(4d$-TM$)$	39	40	41	42	43	44	45	46	47
$Q^{\star}(N)$	7.70	7.79	7.82	7.68	7.62	7.55	7.47	7.38	7.33

FIG. 10. (Color online) The density of states $\rho(E_F)$ at the Fermi energy, and Stoner's enhancement parameter S_F.

V. MAGNETIC PROPERTIES

In Stoner's[52] mean-field theory the succeptibility, at $T=0$ K, is given by

$$\chi_{sp} = \frac{\mu_B^2 \rho(E_F)}{1 - \rho(E_F)I_F}, \tag{4}$$

where μ_B is the Bohr magneton and I_F is a parameter that can be calculated from the energy-band structure of the material. $\rho(E_F)$ is the density of states at the Fermi level. Stoner's condition for the occurrence of ferromagnetism is

$$\rho(E_F) \times I_F \geq 1. \tag{5}$$

In Fig. 10 we show the behavior of the Fermi-level density of states $\rho(E_F)$, and also of the Stoner enhancement, $S_F = [1 - I_F \times \rho(E_F)]^{-1}$, as calculated considering the Stoner parameter as having a constant value $I_F = 0.47$ eV, which is the exchange constant value for MoN as calculated in Ref. 7, along the series. Aside from MoN, these nitrides show moderate enhancements and the paramagnetic state is predicted to be the stable one for the whole series $[\rho(E_F) \times I_F < 1]$.

VI. FINAL REMARKS

The electronic structures of NbN and MoN have been studied in the NaCl structure, by means of the self-consistent augmented plane-wave method (APW), in connection to superconductivity.[7,53] The motivation of these calculations was that high-temperature superconductors usually occur for compounds in the cubic structure. Papaconstantopoulos *et al.*[7] studied MoN looking for a critical temperature T_c higher than that for the hexagonal phase, the more stable one. They expected that the addition of one electron when going from NbN to MoN would move the Fermi level to a region of considerable higher density of states (which is directly related to T_c). Actually they found 1.14 and 0.47 (states/eV spin cell) for MoN and NbN, respectively, indicating $T_c(\text{MoN}) = 30$ K, to be compared to $T_c(\text{NbN}) = 17$ K. Analogous results we found for the zinc-blende phase, 1.13 and 0.75 (states/eV spin cell), respectively, for MoN and NbN

(see Fig. 10). Thus one can expect similar behavior of the zinc-blende compounds in that connection to superconductivity. Obviously one has to take into account the inherent differences between the two structures. For instance, most of the 4d occupied states close to the Fermi level have t_{2g} symmetry in the NaCl structure while e_g symmetry in the zinc-blende phase. On the other hand in both structures these are nonligand states.

Related to the present study total-energy calculations have been carried out for the RhN and PdN compounds using the FP-LAPW method and the gradient generalized approximation (GGA).[54] The results show that the zinc-blende phase is the most stable when compared to the NaCl, CsCl, wurtzite, and NiAs structures.[55]

Zaoui *et al.*[56] performed FP-LAPW calculations, using the same level of computation as ours, for the NaCl structure of Ti, V, Cr, Mo carbides, and Mo nitride. They found a strong charge transfer from Mo to N (around $|1.6e|$, according to our criteria for defining charges). On the other hand, they have found that the DOS curves, besides a first region dominated by the 2s-N states, present a second region characterized by two peaks separated by a minimum of the DOS. The first peak is dominated by the 2p-N states and the second peak, is situated above the Fermi level and is dominated by the 4d-Mo states. Their findings for the NaCl structure are similar to ours for the zinc-blende structure, except that we found a very distinctive gap energy between the referred 2p-N and 4d-Mo regions (this gap decreases along the series; see Fig. 8); this seems to be a clear difference between NaCl and zinc-blende structures. At the beginning of the series the bulk modulus increases as the number of valence electrons increases. This result indicates that the additional electrons contribute in the bonding of the solids and strengthen them. The 4d-Mo states, with contributions of 2p-N, dominate the density of states around the Fermi level. This effect indicates the hardness of these materials; apparently, this fact and the charge transfer greatly influences the bonding in these materials.

Our all-electron results may be used as a reference for discussing the accuracy of eventual calculations based on pseudopotentials as they are typically carried out. Ideally, perfect transferable pseudopotentials would give the same results as all-electron calculations. Contrary to the pseudopotential methods, the FP-LAPW method takes into account the core effects; the widely adopted pseudopotential approach generates calculated data which are found to depend significantly on the treatment of the core states of the metals ions. The accuracy of pseudopotential calculations may be comparable to that of all-electron calculations only if core and semicore states are treated in an appropriate way.[50] Besides, regardless whether LDA or GGA is used, special care has to be taken in generating pseudopotentials in order to achieve an accuracy comparable to that of the all-electron calculations.

The LDA and GGA are expected to have different performances when calculating cohesive and formation energies.[50] Regarding the many available GGA's and LDA, there are both favorable and unfavorable aspects for the III-nitride systems.[50] An analysis of the different GGA functionals shows that the reduction of the cohesive energies is due to

stronger gradient corrections on nonlocality, in particular, in the exchange energy component of these functionals. While the increased nonlocality improves the description of molecular binding energies, results show that it worsens the description of the cohesive energies of the III-nitride systems.[50]

VII. SUMMARY

In summary, we have carried out *ab initio* calculations of the structural, electronic, and magnetic properties of the 4d transition-metal nitrides in the zinc-blende structure, taken as candidates to integrate the fast developing technology of the cubic III nitrides. As they have not yet been fabricated, we anticipate their structural, electronic, and magnetic properties. Their lattice parameters and bulk moduli are foreseen to be larger and smaller, respectively, than in the NaCl-type structure. Their cohesive and formation energies are comparable to those of the respective NaCl phase. We succeeded to adjust power laws for the bulk modulus as a function of the first-neighbors distances. Except for YN, which is insulating, all other nitrides are highly conductive owing to a finite density of states at the Fermi level from the residual electrons contributed by each atom in the metal d band. The energy-band structures and density-of-states curves are interpreted in terms of the filling of the ligand, nonligand, and antiligand states. The internal energy gap between the ligand and antiligand states decreases monotonically along the series. A charge transfer from the metal atom to nitrogen atom is predicted to occur, anticipating a metal-covalent-ionic binding in these compounds. Based on Stoner's model all compounds are predicted to be paramagnetic.

Also, based on our calculations we antecipate that the (4d-TM)N compounds may have practical use in connection to the technology of the cubic III-nitride semiconductors: their useful mechanical properties, as hardness, may be combined to their metallic and their paramagnetic behaviors in the fabrication of contact films having smooth interfaces with the III-nitride materials.

ACKNOWLEDGMENTS

*Email address: rdepaiva@fisica.ufmg.br

[1] V. A. Chitta, J. A. H. Coaquira, J. R. L. Fernandez, C. A. Duarte, J. R. Leite, D. Schikora, D. J. As, K. Lischka, and E. Abramof, Appl. Phys. Lett. **85**, 3777 (2004); M. Marques, L. K. Teles, L. M. R. Scolfaro, L. G. Ferreira, and J. R. Leite, Phys. Rev. B **70**, 073202 (2004); C. G. Rodrigues, J. R. L. Fernandez, J. R. Leite, V. A. Chitta, V. N. Freire, A. R. Vasconcellos, and R. Luzzi, J. Appl. Phys. **95**, 4914 (2004); L. E. Ramos, J. Furthmuller, J. R. Leite, L. M. R. Scolfaro, and F. Bechstedt, Phys. Rev. B **68**, 085209 (2003); L. K. Teles, L. G. Ferreira, J. R. Leite, L. M. R. Scolfaro, A. Kharchenko, O. Husberg, D. J. As, D. Schikora, and K. Lischka, Appl. Phys. Lett. **82**, 4274 (2003).

[2] R. de Paiva, J. L. A. Alves, R. A. Nogueira, J. R. Leite, and L. M. R. Scolfaro, J. Magn. Magn. Mater. **288**, 384 (2005); R. de Paiva, R. A. Nogueira, and J. L. A. Alves, J. Appl. Phys. **96**, 6565 (2004).

[3] P. J. Dismukes, M. W. Yim, and S. V. Ban, J. Cryst. Growth **13-14**, 365 (1972).

[4] H. F. George and H. K. John, Phys. Rev. **93**, 1004 (1954).

[5] H. Nakagawa, S. Nasu, H. Fujii, M. Takahashi, and F. Kanamaru, Hyperfine Interact. **69**, 455 (1991).

[6] K. Suzuki, T. Kaneko, H. Yoshida, H. Morita, and H. Fujimori, J. Alloys Compd. **224**, 232 (1995).

[7] D. A. Papaconstantopoulos, W. E. Pickett, B. M. Klein, and L. L. Boyer, Phys. Rev. B **31**, 752 (1985). As calculated by J. F. Janak [Phys. Rev. B **16**, 255 (1977)]. The values of I_F for the 4d transition-metal elements are almost constant along the series ($I_F \sim 0.3$ eV). We suppose that in the nitrides the trend is the same and adopt the value for MoN as representative of the whole series.

[8] C. S. Sandu, M. Benkahoul, M. Parlinska-Wojtan, R. Sanjines, and F. Levy, Surf. Coat. Technol. **200**, 6544 (2006).

[9] R. Sanjines, M. Benkahoul, C. S. Sandu, P. E. Schmid, and F. Lvy, Thin Solid Films **494**, 190 (2006).

[10] J. E. Sundgren and H. T. G. Hentzell, J. Vac. Sci. Technol. A **4**, 2259 (1986).

[11] W. S. Williams, in *Progress in Solid State Chemistry*, edited by M. Reiss and J. D. Mac Calden (Pergamon, New York, 1971), Vol. 6.

[12] P. Hones, R. Sanjines, and F. Levy, Surf. Coat. Technol. **94-95**, 398 (1997).

[13] R. Sanjines, P. Hones, and F. Levy, Thin Solid Films **332**, 225 (1998).

[14] W. Slysz, M. WJgrzecki, J. Bar, P. Grabiec, M. Gorska, V. Zwiller, C. Latta, P. Bohi, I. Milostnaya, O. Minaeva, A. Antipov, O. Okunev, A. Korneev, K. Smirnov, B. Voronov, N. Kaurova, G. Goltsman, A. Pearlman, A. Cross, I. Komissarov, A. Verevkin, and Roman Sobolewskic, Appl. Phys. Lett. **88**, 261113 (2006).

[15] W. De La Cruz, J. A. Díaz, L. Mancera, N. Takeuchi, and G. Soto, J. Phys. Chem. Solids **64**, 2273 (2003).

[16] N. Takeuchi, Phys. Rev. B **66**, 153405 (2002).

[17] L. Mancera, J. A. Rodriguez, and N. Takeuchi, J. Phys.: Condens. Matter **15**, 2625 (2003).

[18] C. Stampfl, W. Mannstadt, R. Asahi, and A. J. Freeman, Phys. Rev. B **63**, 155106 (2001).

[19] M. Chhowalla and H. E. Unalan, Nat. Mater. **4**, 317 (2005).

[20] A. Fernández Guillermet, J. Häglund, and G. Grimvall, Phys. Rev. B **45**, 11557 (1992).

[21] C. Stampfl, W. Mannstadt, R. Asahi, and A. J. Freeman, Phys.

Rev. B **63**, 155106 (2001).

[22] J. H. Kim and P. H. Holloway, Appl. Phys. Lett. **84**, 711 (2004).

[23] N. Schönberg, Acta Chem. Scand. (1947-1973) **8**, 199 (1954).

[24] N. V. Troitskaya and Z. G. Pinsker, Kristallografiya **6**, 43 (1961).

[25] T. L. Francavilla, S. A. Wolf, and E. F. Skelton, IEEE Trans. Magn. **17**, 569 (1981); N. Pessall, R. E. Gold, and H. A. Johansen, J. Phys. Chem. Solids **29**, 19 (1968).

[26] R. H. Hammond, IEEE Trans. Magn. **11**, 201 (1975).

[27] W. W. Fuller, S. A. Wolf, D. U. Gubser, E. F. Skelton, and T. L. Francavilla, J. Vac. Sci. Technol. A **1**, 517 (1983).

[28] B. Olinger and L. R. Newkirk, Solid State Commun. **37**, 613 (1981).

[29] B. W. Olinger, L. R. Newkirk, and J. C. King, Acta Crystallogr., Sect. A: Cryst. Phys., Diffr., Theor. Gen. Crystallogr. **38**, 151 (1982).

[30] E. Gregoryanz, C. Sanloup, M. Somayazulu, J. Badro, G. Fiquet, H.-k. Mao, and R. J. Hemley, Nat. Mater. **3**, 294 (2004). Subsequently, B. R. Sahu and L. Kleinman (Ref. 31) and M. B. Kanoun and S. Coumri-Said (Ref. 32) performed first-principles calculations of electronic properties of PtN and confirmed that this compound crystallizes in the zinc-blende phase. R. Yu and X. F. Zhang (Ref. 33), also performing *ab initio* calculations, concluded that platinum nitride can be stabilized in the fluorite structure. Recently, other calculations (Ref. 34) investigated the pyrite PtN_2 structure that may explain the experimental observations. Thus the actual structure of platinum nitride remains a puzzle.

[31] B. R. Sahu and Leonard Kleinman, Phys. Rev. B **71**, 041101(R) (2005).

[32] M. B. Kanoun and S. Goumri-Said, Phys. Rev. B **72**, 113103 (2005).

[33] R. Yu and X. F. Zhang, Appl. Phys. Lett. **86**, 121913 (2005).

[34] S. K. R. Patil, S. V. Khare, B. R. Tuttle, J. K. Bording, and S. Kodambaka, Phys. Rev. B **73**, 104118 (2006); R. Yu, Q. Zhan, and X. F. Zhang, Appl. Phys. Lett. **88**, 051913 (2006); Andrea F. Young, Javier A. Montoya, Chrystele Sanloup, Michele Lazzeri, Eugene Gregoryanz, and Sandro Scandolo, Phys. Rev. B **73**, 153102 (2006).

[35] P. Hohenberg and W. Kohn, Phys. Rev. **136**, B864 (1964); W. Kohn and L. J. Sham, Phys. Rev. **140**, A1133 (1965).

[36] P. Blaha, K. Schwarz, G. K. H. Madsen, D. Kvasnicka, and J. Luitz, Techn. Universität Wien, Austria, 2001.

[37] D. M. Ceperley and B. J. Alder, Phys. Rev. Lett. **45**, 566 (1980).

[38] J. P. Perdew and Y. Wang, Phys. Rev. B **45**, 13244 (1992).

[39] E. Sjöstedt, L. Nordsström, and D. J. Singh, Solid State Commun. **114**, 15 (2000).

[40] G. K. H. Madsen, P. Blaha, K. Schwarz, E. Sjöstedt, and L. Nordström, Phys. Rev. B **64**, 195134 (2001).

[41] F. D. Murnaghan, Proc. Natl. Acad. Sci. U.S.A. **30**, 244 (1944).

[42] M. Sigalas, D. A. Papaconstantopoulos, and N. C. Bacalis, Phys. Rev. B **45**, 5777 (1992).

[43] V. Ozolins and M. Korling, Phys. Rev. B **48**, R18304 (1993).

[44] C. D. Gelatt, Jr., A. R. Williams, and V. L. Moruzzi, Phys. Rev. B **27**, 2005 (1983).

[45] B. Eck, R. Dronskowski, M. Takahashi, and S. Kikkawa, J. Mater. Chem. **9**, 1527 (1999).

[46] Pui K. Lam, Marvin L. Cohen, and G. Martinez, Phys. Rev. B **35**, 9190 (1987).

[47] G. Kresse and J. Furthmuller, Phys. Rev. B **54**, 11169 (1996); Comput. Mater. Sci. **6**, 15 (1996).

[48] Juarez L. F. Da Silva, Catherine Stampfl, and Matthias Scheffler, Surf. Sci. **600**, 703 (2006).

[49] M. Fuchs, J. L. F. Da Silva, C. Stampfl, J. Neugebauer, and M. Scheffler, Phys. Rev. B **65**, 245212 (2002).

[50] M. Fuchs, J. L. F. Da Silva, C. Stampfl, J. Neugebauer, and M. Scheffler, Phys. Rev. B **65**, 245212 (2002).

[51] J. Haglund, G. Grimvall, T. Jarlborg, and A. F. Guillermet, Phys. Rev. B **43**, 14400 (1991).

[52] E. C. Stoner, Proc. R. Soc. London, Ser. A **154**, 656 (1936); **169**, 339 (1939).

[53] W. E. Picket, B. M. Klein, and D. A. Papaconstantopoulos, Physica B & C **107**, 667 (1981).

[54] J. P. Perdew, K. Burke, and M. Ernzerhof, Phys. Rev. Lett. **77**, 3865 (1996).

[55] F. Leite, J. L. A. Alves, S. Azevedo, and R. de Paiva (unpublished). We found that the zinc-blende phase is more stable than NaCl, CsCl, wurtzite, and NiAs structures, respectively, by 114, 97, 20, and 58 meV for RhN and by 39, 130, 11, and 98 meV for PdN.

[56] A. Zaoui, S. Kacimi, B. Bouhafs, and A. Roula, Physica B **358**, 63 (2005).